AN EMPIRICAL MODEL FOR GEOEFFECTIVENESS OF HIGH SPEED STREAMS IN SOLAR WIND

DIANA BEŞLIU-IONESCU[1,2], GEORGETA MARIŞ MUNTEAN[2]

[1]*Astronomical Institute of the Romanian Academy, 5, Cutitul de Argint St., 040557 Bucharest, Romania*
[2]*"Sabba S. Ştefănescu" Institute of Geodynamics of the Romanian Academy, 19–21, Jean-Louis Calderon St., 020032 Bucharest, Romania*

We present an empirical model to estimate the probability that a high speed stream produced by a coronal hole will be associated with a geomagnetic storm or not. The model is applied to a database build using the HSS catalogue available on the Institute of Geodynamics webpage at http://www.geodin.ro/hss-sc23/. We present the structure of the catalogue as well as a statistical analysis of these currents. We estimate that the model proposed may correctly predict the association or disassociation of a HSS that is generated by a coronal hole with a geomagnetic storm with a 80% efficiency.

Key words: HSS, geomagnetic storm, empirical modelling.

1. INTRODUCTION

The solar wind is propagating throughout interplanetary space (heliosphere) and interacting with all bodies and structures met in its way; it establishes a complex link between the solar atmosphere and the Earth system. Solar wind structure and properties are changing in space and time, during the 11-year solar cycle depending on the changes of their solar sources. A lot of new knowledge about its structure was brought about after the Skylab era (1973–1974) when coronal holes were discovered as the sources of high speed streams (HSS) in the solar wind.

The best-established solar sources of the HSSs are indeed the coronal holes (CHs), the dark regions in solar corona with open magnetic fields localized specially in the polar regions. Observations from the solar orbiting Ulysses spacecraft (Phillips *et al.*, 1995) have shown a latitudinal dependence of the solar-wind speed: over the poles the wind is fast (~500–800 km s^{-1}), while at lower latitudes the velocities tend towards ~300–400 km s^{-1}. The HSSs produced by coronal holes are recurrent, co-rotating streams, with an apparent tendency to occur at a 27 days interval. It is worth noticing that CHs are also the source of slow wind, which could be emerging from the bordering divergent regions of the holes. Fast wind from such holes catches up with downstream slow solar wind, forming a co-rotating interaction region (CIR) followed by a HSS. Coronal holes can also appear at lower solar latitudes and near equator, either as discrete regions or as long (even trans-equatorial) extensions from a polar coronal hole. Such extended CHs can appear during all phases of the 11-year cycle, but are more noticeable in the descending and minimum phases.

There are also some non-recurrent HSSs produced by eruptive solar phenomena such as: flares, sudden disappearing filaments, eruptive prominences, and coronal mass ejections (CMEs). It is well known that all these eruptive coronal phenomena also produce traveling interplanetary particle fluxes (streams) that, consequently, disturb the heliosphere and the planetary magnetospheres. All these heliospheric "disturbances" are registered as some typical currents in the solar wind. All the fast streams in solar wind could cause geomagnetic storms (GSs), polar auroras and even the geomagnetically induced currents in the large extent terrestrial technological systems. They are also disturbing the space technological systems (Maris, Crosby, 2012).

A series of works identified and analysed the HSSs during the solar cycles (SCs) nos. 20–23. Thus, the works of the Swedish team (Lindblad, Lundstedt, 1981; 1983; 1989) or the Greek team

(Mavromichalaki *et al.*, 1988; Mavromichalaki, Vassilaki, 1998) catalogued these currents in the solar wind for the period of three SCs, nos. 20–22, 1964–1996. HSSs during SC 23 were determined and published by other three co-authors teams (Gupta, Badruddin, 2010; Maris, Maris 2012; Xystouris *et al.*, 2014).

In the current study we refer to high speed streams in the solar wind emitted by coronal holes and the geomagnetic storms triggered as consequences of their impact on the terrestrial magnetosphere. We used HSSs data listed in the HSSs Catalogue (Maris, Maris, 2012) for the solar cycle 23, 1996–2008. HSSs emitted (produced) by CHs that have interacted throughout their duration and propagation with other fast solar particle fluxes (emitted by CMEs, solar flares, eruptive prominences) have not been considered, as well as those that were superimposed on a sectorial boundary of the interplanetary magnetic field.

The terrestrial magnetosphere is a cavity in the solar wind flow formed and structured by the interaction of the solar wind and the interplanetary magnetic field with the intrinsic terrestrial magnetic field and ionized upper atmosphere. This interaction is dominated by the strong intrinsic quasi-dipolar magnetic field of the Earth. So, the terrestrial magnetosphere is a dynamic region of flowing plasma guided by the terrestrial magnetic field, which at times is connected with the Sun's plasma and magnetic field by the solar wind.

Although the general concept on sources of geomagnetic storm has not changed during many years, in the literature on the solar–terrestrial relations there are different estimations of solar and interplanetary events effectiveness to produce geomagnetic storms from 30% up to 100%. For example, estimations of CME geoeffectiveness change from 35–45% up to 83–100%. The reasons of these discrepancies may be due to the differences in used methods for: geomagnetic storm identification, interplanetary space event identification, solar event and its dynamics analysis, and the correlation analysis between geomagnetic, interplanetary and solar events (Yermolaev, Yermolaev, 2005 and the references here in).

The present work applied an empirical model in order to estimate the geoeffectiveness of the HSS produced by CHs.

The following sections describe the data used in this study, its analysis and the empirical model.

2. THE DATA

We used a complex table of data that lists the HSS parameters, dominant magnetic polarity of the interplanetary magnetic field throughout the HSS duration and the data for the geomagnetic storms (a part of this table is seen in Table 1).

Table 1

Example of the list of HSS emitted by CH and their associated geomagnetic storms

Year	Mon	Day	V0 km/s	VMax km/s	Dur days	DVM km/s	IMF	Bz_min nT	Dst_min nT	dt/t, Bz<0	Type
1996	3	9	320.3	571.7	7.2	251.4	-	-8.3	-60	-2h/12h	GC
1996	3	19	379.7	643.7	5	264	-	-5.2	-54	-2h/21h	GC
1996	3	24	423	577.7	3.9	154.7	-	-7.2	-60	-2h/9h	GC
1996	4	13	392.7	604.3	3.1	211.6	-	-7.2	-56	-2h/ 4h	GC
1996	4	16	438.3	714.7	5.9	276.4	-	-3.9	-52	-2h/>12h	GC
1996	9	9	348	665.7	9.4	317.7	+	-4.1	-54	-1h/2h	SSC
1996	9	19	454.3	656.3	5.4	202	+	-3.2	-51	-2h/>8h	GC
1996	9	25	411.3	636.7	4.5	225.4	+	-3.7	-50	-3h/5h	GC
1996	10	21	406.3	642	4	235.7	+	-9.5	-105	-2h/8h	GC
1997	3	24	350	576.3	7.6	226.3	-	-7.5	-63	-4h/19h	GC
1997	4	16	310	541.3	6.9	231.3	-	-9.3	-77	-1h/5h	SSC

Table 1 (continued)

1997	10	23	314.7	539	8.6	224.3	+	-9.2	-64	-2h/5h	SSC
1998	3	9	267.7	543.7	7.4	276	-	-15	-116	-5h/12h	GC
1998	3	20	312.3	601.3	4.8	289	+	-12.6	-85	-2h/8h	GC
1998	4	23	322.7	491.3	6.2	168.6	-	-9.1	-69	-3h/10h	SSC
1998	6	6	369.7	623	5.6	253.3	-	-9.6	-50	-2h/7h	SSC
1998	7	15	305	602	5.2	297	-	-4	-58	-1h/5h	GC
1998	12	24	324.3	517.3	4	193	+	-10	-57	-2h/4h	GC
1999	2	28	339	529.7	3.8	190.7	-	-14.4	-95	-4h/10h	SSC
1999	3	29	325.7	532.3	4.1	206.7	-	-11.1	-56	-2h/3h	SSC
1999	8	15	313	758.7	8.2	445.7	+	-6.4	-56	-6h/14h	SSC
1999	9	9	397	609.3	10.4	212.3	+	-6.3	-74	-4h/12h	SSC
1999	10	9	388	710.7	9.6	322.7	+	-9	-67	-3h/15h	SSC
1999	11	6	335	662.7	9.3	327.7	+	-7.2	-73	-2h/9h	SSC
1999	11	16	314.7	582.7	5.4	268	-	-11.6	-79	-4h/15h	SSC
1999	12	29	349	744.7	11	395.7	+	-2.9	-50	-1h/9h	GC

Columns 1–3 refer to the HSS beginning calendar date (year-month-day), columns 4–7 list HSS parameters (V0 – initial speed, Vmax – maximum speed, duration and DVM = Vmax-V0). Column 8 shows the dominant interplanetary magnetic field polarity. Columns 9–13 list: the minimum negative Bz value recorded before the maximum of the storm (such as defined by the Dst minimum value), Dst_min which is the minimum Dst value, information about the beginning of the storm (SSC – sudden storm commencement, GC – storm with gradual commencement), dt / t, Bz < 0 – the time interval between Bz_min and Dst_min / the number of hours when Bz was negative. The geomagnetic storms that were taken into consideration were the moderate ones (– 100 nT ≤ Dst ≤ – 50 nT) and the intense ones (Dst ≤ – 100 nT). The HSS_GS Complex Catalogue (Maris, Maris, 2010) was used for the association of HSSs with geomagnetic storms, as well as some data (Dst and Bz values and their corresponding times) that were updated to the definitive values of the parameters listed in the OMNI 2 database (http://omniweb.gsfc.nasa.gov/).

3. DATA ANALYSIS

3.1. HIGH SPEED STREAMS EMITTED FROM CORONAL HOLES

Table 2 summarized the yearly distribution of the most intense HSSs considered during SC 23 pointing on the number of HSSs per year (row 3), their maximum velocity (row 4) and the velocity gradient (DVmax = Vmax – V0) in row 5. Rows 7 and 8 present the yearly distribution of the intense geomagnetic storms and those that had a sudden commencement (SSC), respectively.

HSS that produced geomagnetic storms are not uniformly distributed during the solar cycle (third line in Table 2). The solar sources of the HSS are coronal holes (CH), regions where the coronal magnetic field is divergent, distributed in all the corona such that: at maximum activity they are generally limited at polar zones, of higher than 60 latitude, at minimum activity they extend towards medium latitudes, sometimes towards the vicinity of the equator or even trans-equatorial. Solar particle propagation from coronal holes follows a spiral path due to the solar differential rotation. The most efficient solar particles to produce the terrestrial field perturbation are those emitted in the ecliptic vicinity, near the solar equator. That means that at solar minimum activity, HSS may produce more geomagnetic storms (see for example year 1996).

Even though at maximum of solar cycle CH are limited (with some exceptions) to high latitude zones, their compact structure determines certain HSS apparition that in their propagation towards Earth may reach lower heliospheric latitudes perturbing therefore the terrestrial magnetosphere. During such periods, the maximum HSS speeds, as well as the speed gradient, reach high values and geomagnetic perturbations may be induced. This is the case for 1999, 2002–2003 (the fourth and fifth rows

in Table 2). The 2001 year that belongs to the maximum phase of SC 23 presents an unexpected low number of HSS. Considering the

relative sunspot numbers, monthly mean, this year represents a gap between 2000 and 2002, the two maxima of SC 23 (Fig. 1a, b).

Table 2

Characteristics of the HSSs emitted from CHs that produced geomagnetic storms

	1996	1997	1998	1999	2000	2001	2002	2003	2004	2005	2006	2007	2008
Nr. HSS	9	3	6	8	7	2	**10**	**14**	**8**	**9**	4	4	3
Vmax >600km/s	7	–	3	4	2	1	7	10	4	8	3	3	2
DVmax >300km/s	1	–	–	4	–	1	6	5	2	7	3	3	2
Dst< -100	1	–	1	–	–	–	**4**	1	–	1	–	–	–
SSC	1	2	2	**7**	1	2	2	–	3	3	1	2	2
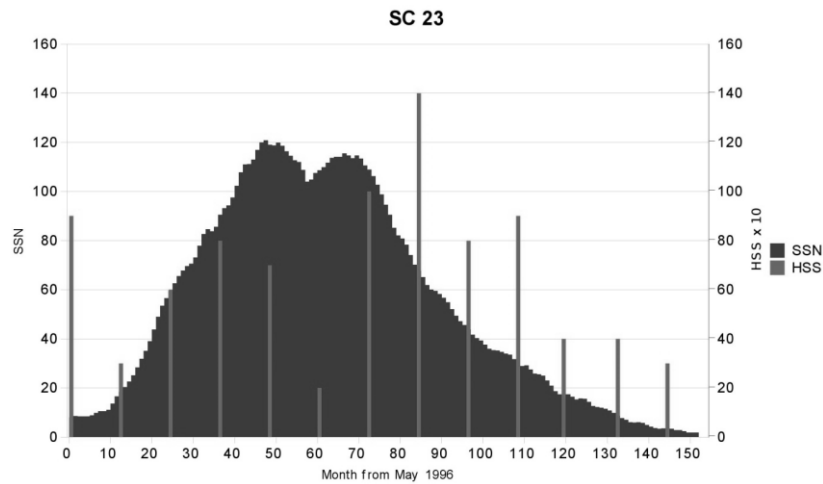
Fig. 1a – SC 23 represented as monthly smoothed means of sunspot number (SSN),
with annual HSS that have produced geomagnetic storms values over plotted.
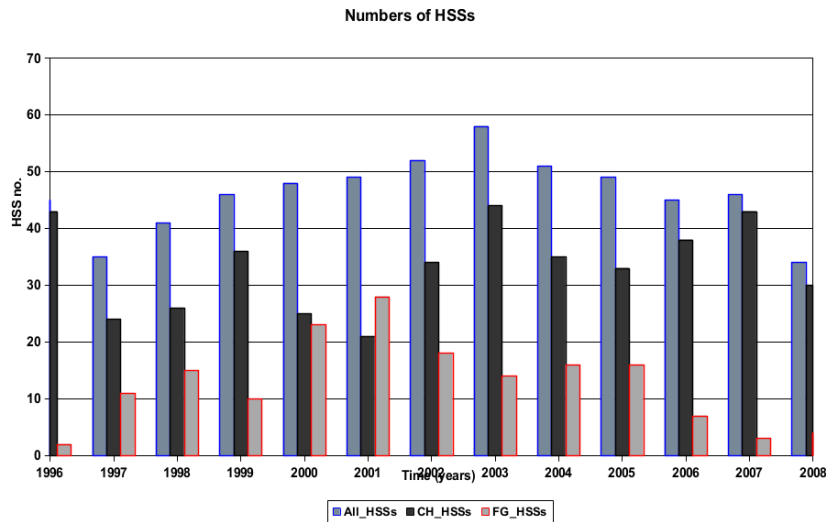

Fig. 1b – Yearly distributions of the HSS number during SC 23 for all HSS (gray histograms),
HSS produced by CH (black histograms) and HSS produced by solar eruptive phenomena (light gray histograms).

We have to say that during 2001 the change of magnetic field polarity for SC 23 took place, and during 2002, there was an intense activity in the HSS productivity, followed by 2003 with the highest activity. On the descending phase of the cycle, until 2005 inclusive, the HSS sustained activity is maintained; that is reflected both by the events number as well as by the maximum speed values of HSS and of the speed gradient.

Year 1996 is part of the SC 23 minimum phase (05.1995 − 05.1997) while years 2006–2008 are contained in the SC 24 minimum phase (02.2006 − 09.2010). We have to remark the low activity of the HSS that produced geomagnetic storms during the prolonged SC 24 minimum phase comparatively with the previous minimum (Maris *et al.*, 2012). Analysing the CH evolutions and structures during the last minimum, we also remark diffuse CH, of small area, unevenly distributed in the mean and low latitude zones, unlike CHs from 1996 when well defined and large CHs were spreading from the polar regions towards and trans the equator.

From the heliographic distribution of CH, the following essential characteristics can be deduced for the HSS geoeffectiveness:

- the HSS emitted from CH situated in the eastern Sun hemisphere, does not perturb the terrestrial magnetosphere (because of the spiral propagation of the solar particles);
- the CH position near the central meridian (± 10°) of the solar disk, assures a HSS geoeffectiveness of ~60%;
- the CH situated in the western hemisphere, produce HSS with a high geoeffectiveness (up to 98%);
- the compact structure and the extended CH area contributes to the HSS energy that can increase the geoeffectiveness.

3.2. GEOMAGNETIC STORMS

The annual distribution of all geomagnetic storms, starting with those of moderate intensity for SC 23, is presented in Fig. 2. We can see that for 2003 there is a maximum for moderate geomagnetic storms, and 2002 for the intense ones.

The structure of the storm beginning shows the existence of a shock wave for those storms that have a sudden commencement (SSC). Their maximum seen in 1999, is due to the complex magnetic structure on the solar corona, when the active regions extensions (through coronal mass ejections for example), favour the shock wave appearance that propagates to the Earth's vicinity.
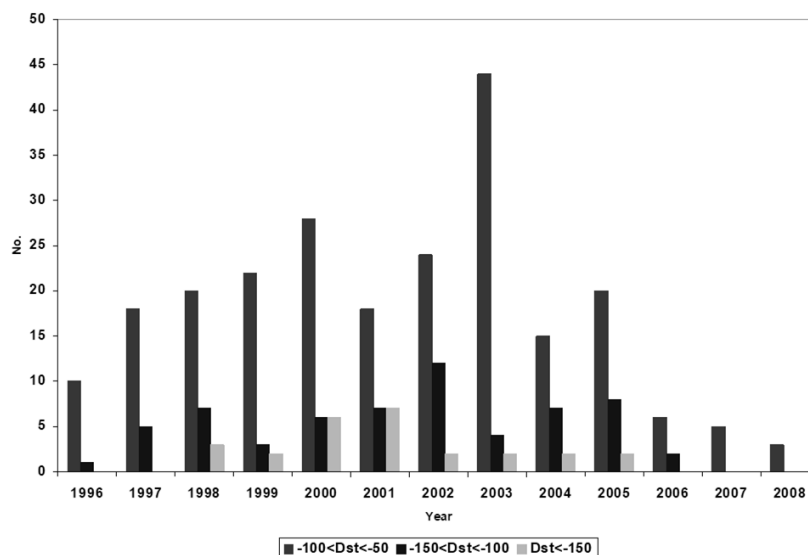

Fig. 2 – Annual distribution of the geomagnetic storms during SC 23 by their intensity (Maris, Maris, 2010, Complex Catalogue: GSs-HSSs, 1996–2008; at: http://www.spacescience.ro/00-old/new1/HSS_Catalogue.html).

The energy transfer from HSS to the terrestrial magnetosphere is induced by magnetic reconnections between the terrestrial field and the interplanetary magnetic field, that appears in front of the magnetosphere when the southern component of the interplanetary magnetic field (Bz) in the GSM coordinate system is negative. Since the IMF is anchored in the solar-wind plasma ("frozen-in flux"), it reaches its maximum at the same time as the plasma density. Both the magnetic field strength and the ion density maximize before the increase in speed while the velocity and the IMF **B**z component show large fluctuations that indicate large amplitude, nonlinear Alfvénic structures that persist for several days. Such structures have important implications for coupling to the magnetosphere (*e.g.* Tsurutani *et al.* 2006). There are differences during CIR (HSS) and CME storms arised from the nature of the IMF. During CMEs there is usually a large, persistent southward turning of the IMF (negative **B**z) accompanied by high solar-wind speed that enhances magnetic reconnection on the dayside, which adds open magnetic flux into the Earth's magnetotail and transfers energy into the system. In comparison CIR do not have extended periods of southward IMF and so the rate of dayside reconnection is much smaller. However, the Alfvénic structures in the solar wind/IMF persist for several days, which suggests that intermittent reconnection occurs over a longer period than during CME storms. This means that energy input to the magnetosphere during a HSS event is comparable to or even greater than the input during a CME event (Kavanagh, Denton, 2007).

Analysing the data regarding the minimum Dst value, the Bz minimum value, the interval that the Bz is maintained negative before and close to the minimum Dst moment, we can see the following:

- the time interval between minimum Bz and minimum Dst is 1–3 hours, with few exceptions when it can be 4 or even 5 hours;
- Bz is maintained negative during several hours, over 5 hours, during most cases (90%) which insures an efficient energy transfer in the magnetosphere, especially in the main phase of the geomagnetic storm

(from the beginning to the minimum Dst time);
- Only 8% of the geomagnetic storms are intense and these are differentiated by the persistence of the Bz negativity during a longer interval (≥ 8 hours).

Analysing the Bz variability comparatively with HSS parameters (Vmax and DVMax), we conclude that a negative Bz insures a greater geoefficiency of a HSS than the speed (energy) of its particles.

4. EMPIRICAL MODEL

The empirical modelling of a certain phenomenon implies establishing some relations that exist between certain experimental data of the analysed phenomena. As such, one needs to gather data relevant to the studied phenomenon, both in respect to statistical evaluation of its behaviour and those referred to its physical nature, where it is possible. Mentioning "data" firstly implies choosing adequate parameters, then establishing some measurements series in time such that the length of the series be relevant to the phenomenon variability (periodicity). The empirical models can be used to establish some mathematical relationships for prognosis of a phenomenon and to underline the tendencies of the studied parameter used. Subsequent data series (or even some older ones that have not been used in empirical modelling) can be used to test models.

We have applied the logistic regression method used by Besliu-Ionescu *et al.* (2019), which is a modified version of the method proposed by Srivastava (2005), and made an attempt to evaluate the probability that a given HSS will be associated with a geomagnetic storm. The method is described in detail in Besliu-Ionescu *et al.* (2019) and it provides a set of regression coefficients that can be used to compute the probability that a HSS will be associated with a geomagnetic storm.

We build a database of HSS using the lists of currents such as listed in the HSS catalogue for solar cycle 23 available at http://www.geodin.ro/hss-sc23. We used the association of HSS with geomagnetic storms done by Maris and Maris

(2010) where the association is between all types of HSS meaning those produced by coronal holes or by eruptive events. The HSS database used here is based on a revised version of the data described above and contains 654 events associated with 596 unique currents.

The logistic regression method needs a set of events to learn from called the training set, and a set to validate it called validation set. We split the database into 2/3 events (436) for the training set and 1/3 events (218) for the validation one, choosing them alternatively.

We used several combinations of the HSS parameters that were described in Section 2. Nine out of eleven regression coefficients obtained using all meaningful parameters (by meaningful we understand any physical measured or computed parameters, excluding therefore dates, times or rotation parameters) were close to zero ($\sim 10^{-8}$–10^{-9}). We then sorted these coefficients and tried many combinations with fewer parameters. We stopped when we obtained coefficients that were not so small and the free coefficient had a similar order as the other coefficients while obtaining acceptable success rates. We defined success a probability that has a value over 0.5 for correctly predicting that a certain HSS is or isn't associated with a geomagnetic storm. Thus, a positive event means the correct prediction of either one of the two situations. Success rates are computed as the ratio between the correct predictions and the total number of events.

Therefore, the combination for the six independent variables that we present here is composed of the initial HSS speed, the maximum speed, the speed gradient, the duration, the minimum value of the southward interplanetary magnetic field and the sectorial boundary of the interplanetary magnetic field. We tried to normalize all measurements, but obtained very small coefficients. Thus we have used the real values for all the speeds, the HSS duration in days, the minimum value of Bz, and a binary variable for the sectorial boundary of the IMF defined as 0 if a cross boundary case and 1 if a positive or negative boundary was observed. This combination had the best success rate for the validation set out of all the parameter combinations that we have used as input.

As for the dependant variable, we have used the minimum Dst value, binned into a binary variable defined as 1 for the HSS with a geomagnetic storm associated and 0 for the HSS that had no geomagnetic storm associated. The programming language used was IDL, in a similar way as Besliu-Ionescu *et al.* (2019).

The summary of the computed regression coefficients is presented in Table 3.

Using this set of coefficients, the probabilities obtained for the association of HSS with geomanetic storm or with no activity are 61% success rate for the training set and 80% success rate for the validation one.

Table 3

Summary of regression coefficients

	Regression Coefficient	Corresponding Value
1	Initial Speed (V0)	-0.9988
2	Maximum Speed (VM)	0.0051
3	Delta V Max (DVM)	-0.0061
4	Duration (dt)	0.0053
5	Minimum Value of Bz (Bz_min)	0.1425
6	Interplanetary magnetic conditions (IMF)	0.0843
7	Free term (b0)	7.6450

5. SUMMARY

- Following CH may give indications for a possible geoeffective HSS with 3–4 days ahead;
- Detecting a solar plasma speed increase

(a HSS) at ACE (from the Lagrangean point L1, 1,500,000 km in front of the magnetosphere) and concomitant analysing the Bz values, makes a geomagnetic storm prediction possible with at least 2 hours before its triggering.

- The non-linear logistic regression method may be used to predict the association of a HSS generated by a coronal hole with a geomagnetic storm.

The empirical model may be improved by extending the database to include other solar cycles or by changing the independent parameter set to include some computed variables that have been proved to have good correlation with the association of geomagnetic storms.

REFERENCES

AKASOFU, S.I. (1981), *Energy coupling between the solar wind and the magnetosphere.* Space Science Review, **28**, pp. 121–190.

BEŞLIU-IONESCU, D., TĂLPEANU, D.C., MIERLA, M., MARIŞ MUNTEAN, G. (2019), *On the prediction of geoeffectiveness of CMEs during the ascending phase of SC24 using a logistic regression method.* Journal of Atmospheric and Solar–Terrestrial Physics, **193**, 105036.

GUPTA, V., BADRUDDIN (2010), *High-Speed Solar Wind Streams during 1996–2007: Sources, Statistical Distribution, and Plasma/Field Properties.* Solar Physics, **264**, pp. 165–188.

KAVANAGH, A., DENTON, M. (2007), *High-speed solar wind streams and geospace interactions.* Astron. & Geophys., **48**, Issue 6, 6.24–6.26, doi:10.1111/j.1468-4004.2007.48624.x.

LINDBLAD, B.A., LUNDSTEDT, H. (1981), *A catalogue of high-speed plasma streams in the Solar wind.* Solar Physics, **74**, pp. 197–206.

LINDBLAD, B.A., LUNDSTEDT, H. (1983), *A catalogue of high-speed plasma streams in the solar wind 1975–1978.* Solar Physics, **88**, pp. 377–382.

LINDBLAD, B.A. LUNDSTEDT, H. (1989), *A third catalogue of high-speed plasma streams in the solar wind – Data for 1978–1982.* Solar Physics, **120**, pp. 145–152.

MAVROMICHALAKI, H., VASSILAKI, A., MARMATSOURI, A. (1988), *A catalogue of high-speed solar-wind streams – Further evidence of their relationship to Ap-index.* Solar Physics, **115**, pp. 345–365.

MAVROMICHALAKI, H., VASSILAKI, A. (1998), *Fast Plasma Streams Recorded Near the Earth During 1985/1996.* Solar, Physics **183**, pp. 181–200.

MARIŞ O., MARIŞ G. (2010), *Complex Catalogue: GSs-HSSs, 1996–2008*; at: http://www.spacescience.ro/00_old/new1/GS_HSS Catalogue.html)

MARIŞ, O., CROSBY, N. (2012), *Space environment effects on space- and ground-based technological Systems*, pp. 293–328, In: *Advances in Solar and Solar-Terrestrial Physics,* Cap. 15, Research Signpost, India, (Editors: G. Maris and C. Demetrescu), ISBN: 978-81-308-0483-5.

MARIŞ, O., MARIŞ, G. (2012), *High speed streams in the solar wind during the 23rd solar cycle*, pp. 97–134, In: *Advances in Solar and Solar-Terrestrial Physics*, Cap. 7, Research Signpost, India, (Editors: G. Mariş and C. Demetrescu), ISBN: 978-81-308-0483-5.

MARIŞ, G., MARIŞ, O., OPREA, C., MIERLA, M. (2012), *High-speed streams in the solar wind during the last solar minimum*, In: Proceedings IAU Symposium, No. 286, 2011, C.H. Mandrini & D.F. Webb Eds. pp. 229–233, doi:10.1017/S1743921312004887.

PHILLIPS, J.L., BAME, S.J., BARNES, A., BARRACLOUGH, B.L., FELDMAN, W.C., GOLDSTEIN, B.E., GOSLING, J.T., HOOGEVEEN, G.W., McCOMAS, D.J., NEUGEBAUER, M., SUESS, S.T. (1995), *Ulysses solar wind plasma observations from pole to pole.* Geophysical Research Letters, **22**, Issue 23, pp. 3301–3304, doi: 10.1029/95GL03094.

SRIVASTAVA, N. (2005), *A logistic regression model for predicting the occurrence of intense geomagnetic storms.* Annalae Geophys., **23**, pp. 2969–2974, http://dx.doi.org/10.5194/angeo-23-2969-2005.

TSURUTANI, B.T., GONZALEZ, W.D., GONZALEZ, A.L.C., GUARNIERI, F.L., GOPALSWAMY, N., GRANDE, M., KAMIDE, Y., KASAHARA, Y., LU, G., MANN, I., McPHERRON, R., SORAAS, F., VASYLIUNAS, V. (2006), *Corotating solar wind streams and recurrent geomagnetic activity: A review.* Journal of Geophysical Research: Space Physics, **111**, Issue A7, CiteID A07S01, doi:10.1029/2005JA011273.

XYSTOURIS, G., SIGALA, E., MAVROMICHALAKI, H. (2014), *A Complete Catalogue of High-Speed Solar Wind Streams during Solar Cycle 23.* Solar Physics, **289**, pp. 995–1012.

YERMOLAEV, YU.I., YERMOLAEV, M.YU. (2005), *Statistic study on the geomagnetic storm effectiveness of solar and interplanetary events.* Advances in Space Research, **37**, Issue 6, pp. 1175–1181.